

Tunable Low-LUMO Boron-Doped Polycyclic Aromatic Hydrocarbons by General One-Pot C–H Borylations

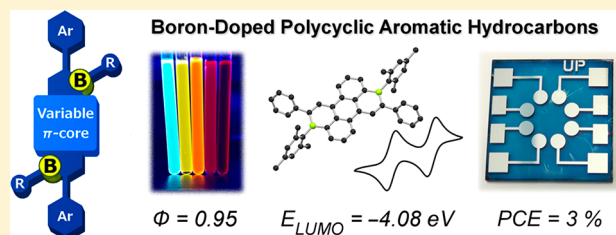
Jeffrey M. Farrell,^{†,§} Carina Mützel,^{†,§} David Bialas,[‡] Maximilian Rudolf,[†] Kaan Menekse,[‡] Ana-Maria Krause,[‡] Matthias Stolte,[‡] and Frank Würthner^{*,†,‡,§}

[†]Institut für Organische Chemie, Universität Würzburg, Am Hubland, 97074 Würzburg, Germany

[‡]Center for Nanosystems Chemistry, Universität Würzburg, Theodor-Boveri-Weg, 97074 Würzburg, Germany

Supporting Information

ABSTRACT: Boron-doping has long been recognized as a promising LUMO energy-lowering modification of graphene and related polycyclic aromatic hydrocarbons (PAHs). Unfortunately, synthetic difficulties have been a significant bottleneck for the understanding, optimization, and application of precisely boron-doped PAHs for optoelectronic purposes. Herein, a facile one-pot hydroboration electrophilic borylation cascade/dehydrogenation approach from simple alkene precursors is coupled with postsynthetic B-substitution to give access to ten ambient-stable core- and periphery-tuned boron-doped PAHs. These include large hitherto unknown doubly boron-doped analogues of anthanthrene and triangulene. Crystallographic, optical, electrochemical, and computational studies were performed to clarify the effect of boron-doped PAH shape, size, and structure on optoelectronic properties. Our molecular tuning allowed the synthesis of molecules exhibiting visible-range absorption, near-unity fluorescence quantum yields, and, to our knowledge, the most facile electrochemical reductions of any reported ambient-stable boron-doped PAHs (corresponding to LUMO energy levels as low as fullerenes). Finally, our study describes the first implementation of a precise three-coordinate boron-substituted PAH as an acceptor material in organic solar cells with power conversion efficiencies (PCEs) of up to 3%.



INTRODUCTION

Graphene¹ and related “nanographene”² substructures have captivated chemists and physicists with their unique structural, (opto-)electronic, and magnetic properties. Concurrently, intense research has surrounded the incorporation of boron into these and related polyaromatic hydrocarbon (PAH) scaffolds.³ The substitution of sp^2 -hybridized carbon for neutral, three-coordinate boron renders these scaffolds electron-deficient owing to the empty p orbital of boron. This “doping” allows manipulation of the electronic, photo-physical, and magnetic properties of polyaromatic systems without compromising their planar geometries. Such boron doping has been championed as a way forward for the band gap manipulation of graphene^{3d} and for the development of n-type organic semiconductors.^{3a,b,4}

Despite great promise, significant obstacles exist for boron-doped PAHs as a class of materials. Namely, difficult syntheses have impeded their study. This is especially true of boron-doped polybenzenoid π -scaffolds bearing only boron and carbon⁵ for which very few general syntheses are known.^{5j–l,6} These represent substructures and potential building blocks of boron-doped graphene.⁷ The synthetic challenges of boron-doped polybenzenoid PAHs have been detrimental to the diversity of available structures and have hampered the focused tuning of properties. Although some examples have been used in organic electronics,^{5h,n,o,8} this class of molecules has yet to match the appealing properties and low LUMO levels of more

extensively used acceptors in organic electronics and photovoltaics (e.g., fullerenes or rylene diimides).⁹

We have recently reported the synthesis of an ambient-stable doubly boron-doped perylene **4a** (Table 1)¹⁰ using the chemistry of cationic three-coordinate boron compounds (borenium ions).¹¹ Our newly devised one-pot reaction sequence entailed N-heterocyclic carbene (NHC) borenium hydroboration, ring-closing dehydrogenative electrophilic borylation, TEMPO-mediated dehydrogenation and hydrolysis.¹² This facile synthesis from a simple, readily accessible alkene precursor contrasted starkly with traditionally difficult boron-doped PAH syntheses. We anticipated that, if applicable to other alkenes, this approach would allow the synthesis and study of boron-doped polybenzenoid systems of varying sizes, boron substitution patterns and periphery substitutions (Figure 1). Herein, we have used this method to synthesize a series of boron-containing PAHs including large and unprecedented doubly boron-doped anthanthrenes and triangulenes. Furthermore, we have succeeded in subsequent postsynthetic substitutions of boron-bound hydroxyl groups for mesityl groups. We have studied the effects of structural changes on photophysical properties, electrochemical properties, and solid-state packing through experimental and computational means. Through structural tuning, we report

Received: May 1, 2019

Table 1. One-Pot Syntheses of Polyaromatic Borinic Acids^c

alkene	product	yield
		1, 49%
		2, 39%
		3, 31%
		4a, 24% ¹⁰ (R = C ₆ H ₅)
		4b, 12% ^{a,b} (R = C ₆ F ₅)
		5, 22% ^b
		6, 15% ^b

^aPerformed in *o*-C₆H₄Cl₂ with step 2 carried out at 160 °C for 24 h and hydrolytic workup by acidic aqueous extraction. ^bStep 2 carried out for 4 h and step 3 carried out for 24 h. ^cIsolated yields. Unless otherwise indicated, reactions performed in C₆H₅Cl with step 2 carried out at 110 °C for 5 h, step 3 carried out at 80 °C for 36 h, and hydrolytic workup by silica gel chromatography.

ambient-stable boron-doped PAHs with fluorescence quantum yields as high as 95% and facile electrochemical reductions representative of LUMO energies comparable to fullerenes. Most importantly, our lowest-LUMO energy boron-doped PAH could be exploited in organic thin-film transistors (OTFTs) with n-type charge carrier mobility and in inverted bulk-heterojunction (BHJ) solar cells with power conversion efficiencies of up to 3%.

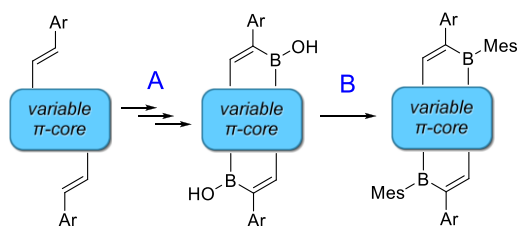


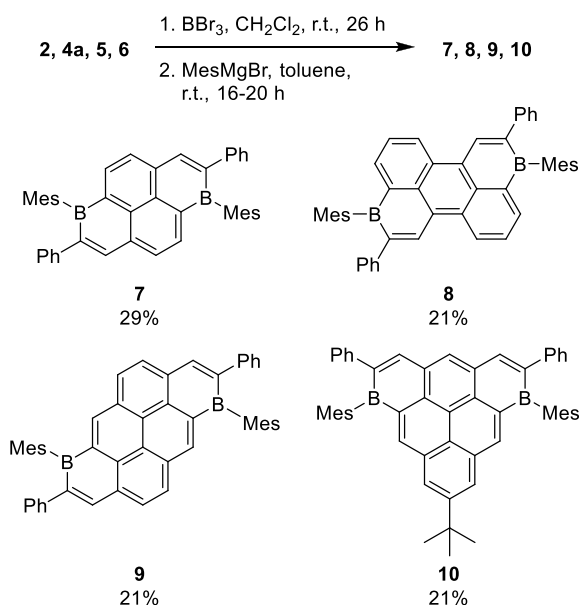
Figure 1. Approach herein for the synthesis of boron-doped PAHs by (A) one-pot hydroboration/electrophilic borylation cascade/dehydrogenation, and (B) mesityl substitution at the boron centers.

RESULTS AND DISCUSSION

Synthesis of Compounds 1–10. All alkene precursors used in our study were synthesized by straightforward Mizoroki–Heck reactions (see [Supporting Information](#)). Conveniently, our one-pot reaction conditions could be used largely unchanged¹⁰ for the synthesis of polyaromatic borinic acids 1–3, 5 and 6 from their respective alkene precursors (Table 1). Each of these precursors was added to a solution of an NHC-borenium salt, which was generated in situ by the combination of HNTf₂ and an air- and moisture-stable NHC-borane adduct¹³ at room temperature in chlorobenzene. Each reaction was then stirred at 110 °C for 4–5 h to effect hydroboration and electrophilic borylation reactions. For electron-deficient fluorinated substrate 4b this step required a longer reaction time at higher temperature in *o*-dichlorobenzene. For each synthesis, dehydrogenation was effected by reaction with a TEMPO radical solution at 80 °C for 24–36 h. Hydrolytic workup allowed the isolation of the desired polycyclic borinic acid products by silica gel chromatography (1–3, 5–6) or acidic aqueous extraction (4b). 1-Boraphenylene 1 (49%),¹⁴ 1,6-diborapyrene 2 (39%), 1,8-diborapyrene 3 (31%), 3,9-diboraperylene 4b (12%), 1,7-diboraanthanthrene 5 (22%), and 2,8-diboratriangulene 6 (15%) (Table 1) were characterized by multinuclear NMR spectroscopy and HRMS (see [Supporting Information](#)). Compounds 1–6 show no signs of degradation when stored as solids under ambient conditions for months. The larger compounds 5 and 6, however, show signs of degradation by ¹H NMR spectroscopy in aerobic solutions within days to weeks (especially upon exposure to ambient light). Although all-carbon triangulene is a notoriously unstable ground state diradical,¹⁵ the core of compound 6 is isoelectronic with a triangulene dication and is therefore reasonably stable.

We envisioned that postsynthetic substitution of the B-hydroxyl moiety would offer even further flexibility to our synthetic approach. We therefore probed borinic acids 2, 5, 6, and previously reported 4a for substitution of B-hydroxyl groups with commonly encountered B-mesityl groups. These borinic acids were each reacted with BBr₃ at room temperature for 26 h, concentrated in vacuo, and subsequently reacted with mesityl magnesium bromide for 16–20 h in toluene to give compounds 7–10 (21–29%) after workup and column chromatography (Scheme 1). Compounds 7–10 were characterized by multinuclear NMR spectroscopy and HRMS (see [Supporting Information](#)). Compounds 7–10 are all ambient stable and compounds 9 and 10 show improved stability compared to their precursors 5 and 6. Compounds 7–10 also show markedly increased solubility in halogenated solvents compared to their respective borinic acid precursors. The success of this synthetic method implies that our borinic acids can be used as synthetic equivalents of boron-doped, all-

Scheme 1. Synthesis of B-Mesityl Boron-Doped PAHs



sp^2 -hybridized polybenzenoid frameworks (i.e., potential precursors for the bottom-up construction of boron-doped graphitic structures).

Crystallographic Studies. Crystals suitable for X-ray crystallography could be obtained from DMSO solutions of **2** and **4b**, a dioxane solution of **5**, and a solution of **8** in 1:1 dichloromethane/hexanes. For all compounds investigated by X-ray crystallography, structures confirm expected connectivity and agree well with optimized structures obtained by DFT calculations at the B3LYP/6-31++G** level of theory (see [Supporting Information](#)). All of the examined π -systems are planar and boron retains trigonal planar geometry with sums of

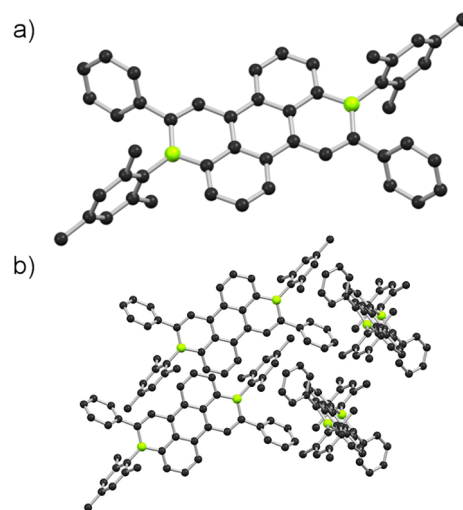


Figure 3. Solid-state structure (a) and packing (b) of **8**. C: black, B: yellow-green. H atoms omitted for clarity.

bond angles about boron of 360° (Figures 2 and 3). Hydrogen bonding is observed between the borinic acid protons of **2**, **4b**, and **5** and cocrystallized coordinating solvents rather than solvent coordination to boron. This characteristic is shared by borinic acid **4a**.¹⁰

Accessible π -surfaces are observed in the solid-state structures of **2**, **4b**, and **5**. These compounds form continuous π -stacks (Figure 2b,e,h). The smallest of the series, **2**, shows interplanar distances of 3.2 Å but with severely slipped stacking and little overlap of π -systems (Figure 2b,c). On the other hand, the solid-state π -stacks of **4** exhibit columnar structures with considerable overlap of π -systems and interplanar distances of 3.4 Å (Figure 2e,f). The C–H for C–F substitution of **4b** has relatively little impact of the solid-

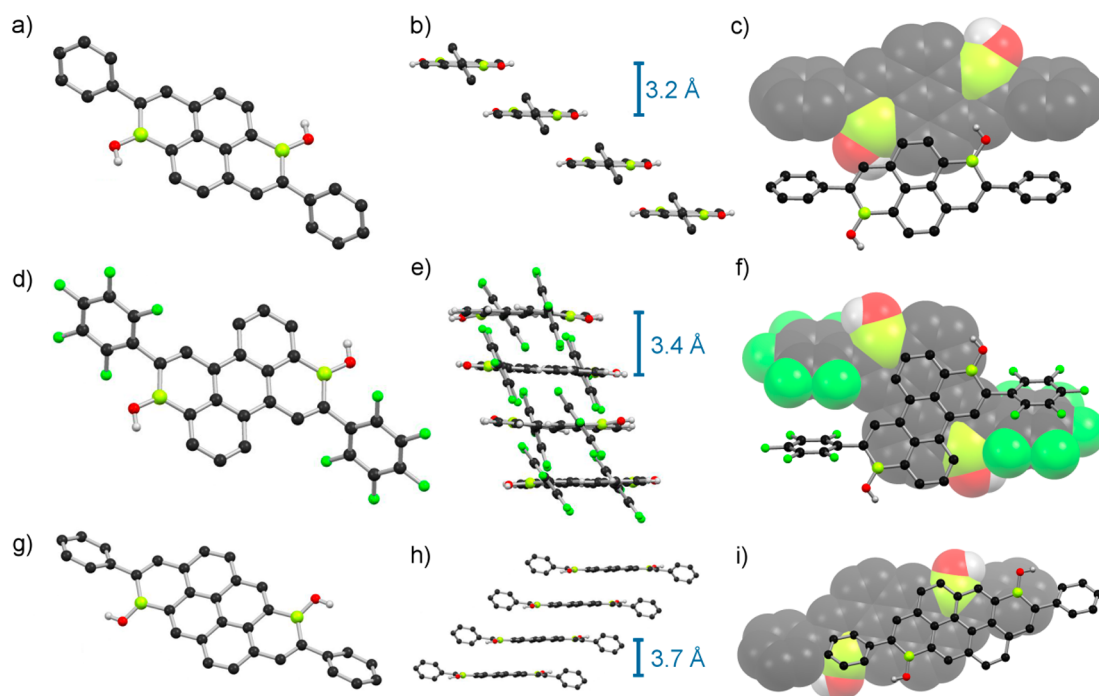


Figure 2. Solid-state structures of **2** (a), **4b** (d), **5** (g), solid-state packing of **2** (b), **4b** (e), **5** (h), and a top-down view of two stacked molecules of **2** (c), **4b** (f), **5** (i). C: black, B: yellow-green, O: red, F: green, H: gray. Solvent molecules and selected H atoms omitted for clarity.

Table 2. Optoelectronic Properties of Boron-Containing Polyaromatic Compounds 1–10 and PC₆₁BM^g

compound	λ_{abs} [nm] (ϵ [M ⁻¹ cm ⁻¹])	λ_{em} [nm]	Stokes shift [cm ⁻¹]	Φ	lifetime τ_1 [ns]	first $E_{1/2 \text{ red}}$ [V]	second $E_{1/2 \text{ red}}$ [V]
1 ^a	374 (8800), 348 (9600)	489	6290	0.27	6.4	-1.98 ^{cd}	–
2 ^a	425 (17 500), 383 (12 700)	561	5700	0.44	7.1	-1.47 ^{cd}	-1.84 ^{cd}
3 ^a	466 (11 600), 358 (6800)	586	4390	0.51	5.9	-1.46 ^{cd}	-1.82 ^{cd}
4a ^{a,10}	560 (23 700), 524 (18 600)	601	1220	0.63	5.4	-1.30 ^{cd}	-1.64 ^{cd}
4b ^a	540 (26 800), 504 (19 300), 473 (8400)	563	760	0.95	6.2	-1.13 ^{cd}	-1.47 ^{cd}
5 ^b	525 (32 600), 491 (26 400), 433 (12 400)	548, 586	800	0.35	3.2	-1.39 ^{cd}	-1.70 ^{cd}
6 ^b	547 (5900), 509 (8800), 479 (9300), 450 (7800), 377 (24 100)	573, 619	830	0.42	6.0	-1.53 ^{cd}	–
7 ^b	467 (14 100), 411 (14 600)	635	5660	<0.01	4.2	-1.15 ^e	-1.62 ^e
8 ^b	611 (31 900), 417 (10 100)	668	1400	0.74	5.6	-1.07 ^e	-1.41 ^e
9 ^b	575 (34 700), 541 (28 800), 455 (19 600)	622	1310	0.28	2.6	-1.17 ^e	-1.51 ^e
10 ^b	591 (5100), 550 (7200), 434 (22 600), 404 (37 200)	633, 684	1120	0.34	2.9	-1.34 ^e	–
PC ₆₁ BM ^{c,9b}	695, 492, 430, 328	–	–	–	–	-1.17 ^f	-1.55 ^f

^aOptical measurements carried out at 298 K in CHCl₃. ^bOptical measurements carried out at 298 K in CH₂Cl₂. ^cOptical measurements carried out at 298 K in cyclohexane. ^dElectrochemical measurements carried out at 298 K in 0.1 M *n*-Bu₄NPF₆ in DMSO. ^eElectrochemical measurements carried out at 298 K in 0.1 M *n*-Bu₄NPF₆ in CH₂Cl₂. ^fElectrochemical measurements carried out at 298 K in *n*-Bu₄NPF₆ 0.1 M *o*-dichlorobenzene. ^gSee Supporting Information for all measurement details. Electrochemical reduction potentials were calibrated with ferrocene as an internal standard and are referenced vs Fc⁺⁰.

state structure, which is remarkably similar to previously reported compound 4a.¹⁰ For compound 5, which bears the largest π -system, π -stacking is observed with larger interplanar distances of 3.7 Å (Figure 2h,i). In this case, periphery phenyl groups are positioned on top of neighboring diboraanthanthrene cores and impede closer packing. Nevertheless, accessible π -surfaces and solid-state π -stacking are not commonly encountered for ambient-stable boron-doped PAHs.^{5a,8a,b} This molecular design possibility may be attractive for organic electronic applications where charge carrier transport is desired along closely stacked π -scaffolds. Conversely, π -stacking is not observed for 8, which bears sterically demanding boron-bound mesityl groups oriented orthogonal to its π -system (Figure 3b). Clearly the steric demands of this mesityl substitution prevents the close approach of π -systems of neighboring molecules of 8.

Redox Properties. Suitably low LUMO energy levels are crucial for application of small molecules as acceptor materials in organic electronics. Electrochemical reduction potentials of boron-doped polyaromatic structures, although more positive than their undoped parent hydrocarbon structures,^{3a} have not yet been reported at levels corresponding to common acceptor compounds such as PC₆₁BM ($E_{1/2} = -1.17$ V vs Fc⁺⁰, 0.1 M *n*-Bu₄NPF₆ *o*-dichlorobenzene,^{9b} $E_{\text{LUMO}} = -3.99$ eV).¹⁶ Moreover, strategies to tune this property are not well established given relatively few examples. In order to address these issues, the electrochemical properties of compounds 1–10 were studied by cyclic voltammetry in 0.1 M *n*-Bu₄NPF₆ DMSO solution (1–6) or in 0.1 M *n*-Bu₄NPF₆ dichloromethane solution (7–10) based on solubility. For singly boron-doped compound 1, a single, reversible reduction could be observed at -1.98 V (Table 2). This first reduction occurs at the most negative potential of all compounds studied. This is somewhat unsurprising given both its onefold (vs twofold) boron doping and its small π -scaffold size for electron delocalization.

For doubly boron-doped borinic acids 2–5 and mesityl derivatives 7–9, two reversible one-electron reductions could be observed with first reductions occurring at much more positive potentials between -1.07 V (8) and -1.47 V (2) (Table 2). Diboraperylene 8 is, to our knowledge, the most

readily reduced ambient-stable core boron-doped PAH yet reported. Doubly boron-doped triangulenes 6 and 10 each exhibited only one reversible reduction at -1.53 V and -1.34 V, respectively. Second reductions for 6 and 10 were irreversible and occurred at -2.17 V and -2.09 V, respectively. The C₆F₅-substituted borinic acid 4b exhibits a first reduction at -1.13 V, which is 0.17 V more positive than its C₆H₅ analogue 4a. Mesityl compounds 7–10 also exhibit more positive reduction potentials than their respective borinic acid precursors 2, 4a, 5, and 6 by between 0.19 and 0.32 V. Presumably, lone-pair donation from borinic acid oxygen atoms to the empty p orbital of boron impedes reduction. These examples show that both our pre- and postsynthetic periphery substitutions are viable methods to predictably tune the electron-accepting ability of boron-doped PAHs. The changes to reduction potentials occur as anticipated, with the substitution of more donating groups for more electron withdrawing groups leading to more positive reduction potentials.

It is worth noting that the periphery substitution of C₆H₅ for C₆F₅ in 4b has a comparable effect on reduction potential ($\Delta E_{1/2} = +0.17$ V vs 4a) to the B–OH for B-mesityl substitution of 8 ($\Delta E_{1/2} = +0.23$ V vs 4a). Indeed, both 4b and 8 exhibit comparable or more facile reductions than PC₆₁BM (Figure 4) and both compounds are ambient-stable. However, 4b possesses accessible π -surfaces evidenced by solid state π -stacking whereas 8 does not (Figure 2e, 3). These results

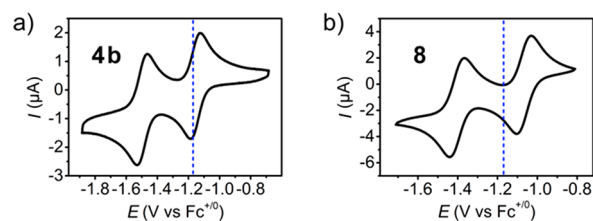


Figure 4. Cyclic voltammograms of (a) 4b (7×10^{-4} M in 0.1 M *n*-Bu₄NPF₆ DMSO, 298 K) and (b) 8 (3×10^{-4} M in 0.1 M *n*-Bu₄NPF₆ CH₂Cl₂, 298 K). Dotted blue lines indicate the potential of the first reduction of PC₆₁BM in 0.1 M *n*-Bu₄NPF₆ *o*-dichlorobenzene.^{9b}

suggest that, even when the diboraperylene scaffold is rendered electron-deficient, steric protection of boron is not a prerequisite for ambient stability. Furthermore, π -stacking, which is often useful for charge-carrier transport in n-type semiconductor materials, is attainable while retaining low LUMO energy levels and ambient stability. In addition, larger variations in reduction potentials are observed within the series of similarly substituted borinic acids of different shapes and sizes (1–3, 5–6, 4a) than for B–OH vs B-mesityl substitution (Table 2). This suggests that careful choice of the core boron-doped π -structure is more important for reduction potentials than the choice of hydroxyl vs mesityl substituents at boron.

With this in mind, investigation of the impact of the core structure on electrochemical behavior is a critical point. Thus, a comparison can be made between 2, 4a, and 5, which are each similarly substituted. The core of each of the three molecules differs in size from the smallest diborapyrene 2 to diboraperylene 4a to the largest diboraanthanthrene 5. Notably, the most readily reduced species is the intermediate case, diboraperylene 4a. Clearly, the electrochemical reduction potentials of boron-doped PAHs are not solely dominated by either π -scaffold size (for charge delocalization) or the ratio of boron to carbon within the π -scaffold (for a greater proportion of formally empty p orbitals). Importantly, this warns against the arbitrary pursuit of large or excessively boron-doped structures as targets for electron acceptor small molecules. Notwithstanding, our calculations of the adiabatic electron affinities¹⁷ of 2, 4a, and 5 at the B3LYP/6-31++G** level of theory (1.84, 2.09, and 2.01 eV, respectively) correctly correspond to the order of experimentally obtained first reduction potentials for the series. Such calculations may therefore provide insight into the most promising future targets for boron-doped polyaromatic core structures in terms of electron-accepting capability.

Compounds 6 and 10 present a striking example of π -scaffold shape as a critical factor for the electrochemical behavior of boron-doped PAHs. Diboratriangulenes 6 and 10 offer a π -core isoelectronic with the dication of triangulene, their isostructural all-carbon parent compound. Therefore, the two-electron reduction products of 6 and 10 should possess dianionic cores that are both isostructural and isoelectronic with triangulene (for which a closed-shell Lewis structure cannot be formulated). Notably, 6 and 10 were the only compounds studied where the second measured electrochemical reductions were irreversible. Considering the notorious instability of the parent triangulene hydrocarbon (which eluded isolation until 2017),¹⁵ our observations of irreversible second reductions suggest the formation of unstable non-Kekulé diboratriangulene dianions at moderate potentials (−2.17 V and −2.09 V vs Fc^{+/0}).

Optical Properties. For many prospective applications of boron-containing PAHs, such as in OLEDs or as molecular sensors, absorption and emission characteristics are important. In organic photovoltaic applications, acceptor materials with visible range absorption are advantageous over fullerene-based competition whose weak visible-range absorption is suboptimal for solar-light harvesting.^{9a} Compounds 1–10 were therefore studied by UV–vis absorption and fluorescence spectroscopy in dichloromethane or chloroform solution (Figure 5). The lowest energy absorption maxima for the series of boron-doped polyaromatics span from the UV for the smallest compound 1 ($\lambda_{\text{abs}} = 374$ nm, Figure 5a) to the long wavelength absorption of compound 8 ($\lambda_{\text{abs}} = 611$ nm, Figure 5b). Extinction

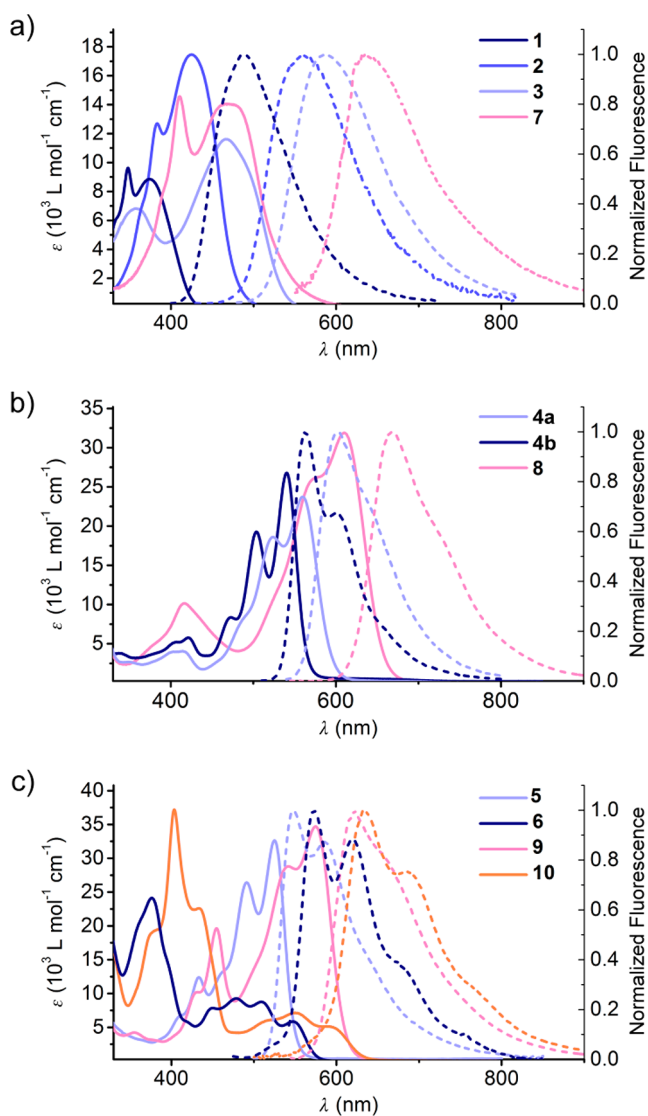


Figure 5. UV–vis absorption (solid lines: 1–4 10^{-5} M in CHCl₃, 298 K; 5–10 10^{-6} to 10^{-5} M in CH₂Cl₂, 298 K) and fluorescence (dashed lines: 1–4 10^{-5} M in CHCl₃, 298 K; 5–10 10^{-7} to 10^{-4} M in CH₂Cl₂, 298 K) spectra of boron-containing PAHs.

coefficients for the absorption maxima of 1–10 range from 9600 M⁻¹ cm⁻¹ (1) to 37 200 M⁻¹ cm⁻¹ (10) (Table 2).

Compounds 1–10 exhibit fluorescence in solution with quantum yields ranging from very poor to excellent; however, most are moderate to good (Table 2). Emission maxima for the series also span a broad range of wavelengths from a blue emission for the smallest compound 1 ($\lambda_{\text{em}} = 489$ nm) to a deep red emission for compound 8 ($\lambda_{\text{em}} = 668$ nm) that extends into the NIR. Fluorescence lifetimes of 1–10 range from 2.6 ns (9) to 7.1 ns (2). The longest wavelength absorption and emission maxima of compounds 2–5 and 7–9 are all significantly red-shifted compared to their parent hydrocarbons pyrene ($\lambda_{\text{abs}} = 335$ nm, $\lambda_{\text{em}} = 385$ nm),¹⁸ perylene ($\lambda_{\text{abs}} = 436$ nm, $\lambda_{\text{em}} = 468$ nm)¹⁹ and anthanthrene ($\lambda_{\text{abs}} = 433$ nm, $\lambda_{\text{em}} = 437$ nm).²⁰ Compounds 1, 2, 3, and 7 also emit in the solid state with $\lambda_{\text{em}} = 530$ nm ($\Phi = 0.10$), $\lambda_{\text{em}} = 566$ nm ($\Phi = 0.05$), $\lambda_{\text{em}} = 643$ nm ($\Phi = 0.03$), and $\lambda_{\text{em}} = 670$ nm ($\Phi = 0.03$), respectively. These emissions, ranging from green to red, are bathochromically shifted with respect to solution-phase emissions of the same compounds. No

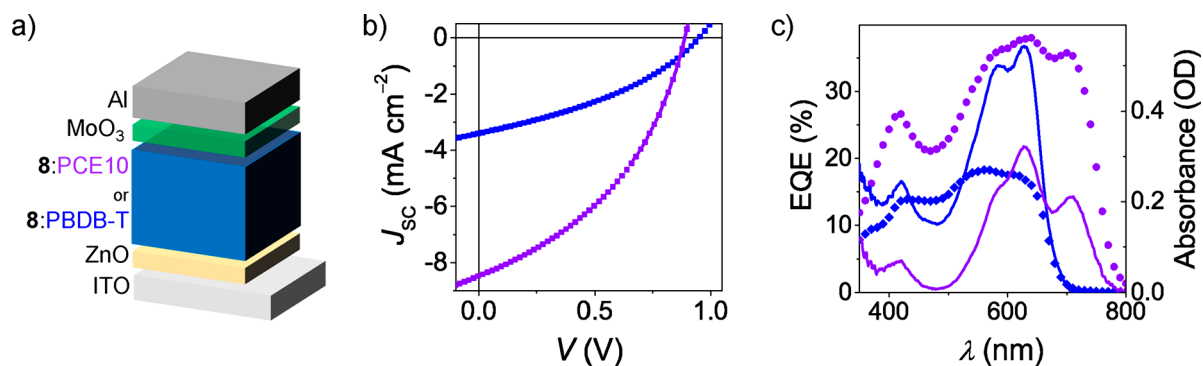


Figure 6. (a) Device configuration of BHJ solar cells investigated herein (ITO/ZnO (30 nm)/8:polymer (1:1)/MoO₃ (10 nm)/Al (100 nm)). (b) J - V characteristics of the inverted BHJ solar cells based on **8** in 1:1 mixing ratio with donor polymers PBDB-T (blue) or PCE10 (violet) under 1000 W/m²AM 1.5G illumination measured in inert conditions. (c) UV-vis absorption (solid line) and EQE (symbols) spectra of inverted BHJ solar cells.

measurable solid-state luminescence was observed for **4**–**6** or **8**–**10**.

The arrangement of boron atoms within the core impacts photophysical properties. This is illustrated by the absorption and emission maxima of **3**, which are bathochromically shifted with respect to those of **2** (Figure 5a). These isomers differ only by the positioning of the B–OH moieties of the diborapyrene core. In compound **3** the electron-rich alkene-like residues are segregated to one side of the π -core opposite to the electron-accepting boron centers. This modification increases the HOMO energy level (see Supporting Information for calculations) effectively reducing the optical bandgap with respect to **2**. TD-DFT calculations reproduce the observed bathochromic shift of the UV-vis absorption spectrum of **3** compared to that of **2** (Figure S112 and Table S15). Notably, these two molecules possess nearly identical first and second reduction potentials (and correspondingly identical calculated LUMO energies). This suggests that arrangement of boron within the π -core may be used to tune the absorption and emission properties of a boron-containing PAH without necessarily changing reduction potentials. Periphery substitutions also significantly affect photophysical properties. All examined mesityl-substituted compounds (**7**–**10**) exhibit bathochromically shifted absorption and emission spectra compared to their parent borinic acids **2**, **4a**, **5**, and **6** (Figure 5b,c). This mesityl substitution has relatively little impact on the fluorescence quantum yields for these compounds except for **7** where it is severely diminished ($\Phi < 0.01$, Table 2) with respect to **2**. On the other hand, the C₆F₅ for C₆H₅ substitution of compound **4b** versus **4a** leads to hypsochromically shifted absorption and emission spectra (Figure 5b). Compound **4b** exhibits a small Stokes shift (760 cm⁻¹) and a well-resolved vibronic progression compared to most other compounds studied (Figure 5b). This simple modification also leads to a marked increase of the fluorescence quantum yield ($\Phi = 0.95$) concomitant with a slightly longer fluorescence lifetime ($\tau_1 = 6.2$ ns) than parent compound **4a** ($\Phi = 0.63$, $\tau_1 = 5.4$) (Table 2). These data suggest inhibition of nonradiative deactivation by this C₆F₅ substitution. Comparing compounds **4b** and **7**–**10**, the B-mesityl substitutions produced bathochromically shifted absorption and emission spectra while the C₆F₅ substitution gave hypsochromically shifted spectra. Since both of these periphery modifications facilitate electrochemical reduction, it appears that photophysical and electrochemical

properties are independently modifiable. The substituent effects on the hypsochromic or bathochromic shifts of UV-vis absorption spectra agree well with those predicted by TD-DFT calculations (Figures S112–S114 and Table S15).

Organic Thin-Film Transistors and Solar Cells. The pursuit of nonfullerene acceptors for organic photovoltaics is an ongoing area of research that hopes to improve upon the fullerenes' low open-circuit voltages, poor solubility, challenging structural modifications and suboptimal light-harvesting abilities.^{9a,d} Although the inclusion of three-coordinate boron into an otherwise all-carbon π -scaffold is a known LUMO energy-lowering modification, well-defined boron-doped PAHs demonstrating this principle have not yet been reported as acceptor materials in organic photovoltaics.^{21,22} Nevertheless, we were inspired to assess **8** in this role due to its good solubility in organic solvents, strong visible-range absorption into the NIR, and its low LUMO energy level comparable to commonly used PC₆₁BM.

To explore this possibility we first probed the charge carrier transport properties of **8** by fabricating organic thin-film transistors (OTFTs, see Supporting Information). Vacuum-processed devices exhibit n-type charge carrier transport with electron mobilities of up to 3×10^{-3} cm² V⁻¹ s⁻¹ on Si/SiO₂/AlO_x/TPA substrates measured under inert conditions (Figures S115, S116, and Table S16). Although these values are modest, they rank favorably among the few strictly three-coordinate boron-doped PAHs reported as n-type semiconductors in OTFTs,^{5n,8a,c} particularly for an amorphous material (see AFM image: Figure S116).

After verifying the ability of **8** to mediate electron transport, we tested **8** as a small-molecule acceptor in solution-processed bulk-heterojunction (BHJ) solar cells with a simple inverted device architecture (ITO/ZnO/8:polymer/MoO₃/Al, Figure 6a). The active layer was processed by spin-casting 1:1 blends of **8** and donor polymers PBDB-T or PCE10 (Figure S117) in 3 vol % 1,8-diiodooctane/chlorobenzene. To our delight, these devices provided power conversion efficiencies (PCEs) of up to 3% with appreciably high open circuit voltages (V_{OC}) up to 0.94 V (Figure 6b,c and Table 3). Furthermore, the wavelength-dependent external quantum efficiencies demonstrate that both the donor polymer and the boron acceptor contribute to the harvesting of solar light (Figure 6c, S119). This proof of concept introduces precise three-coordinate boron-doped PAHs as a new class of nonfullerene acceptors for prospective use in organic solar cells.

Table 3. Organic BHJ Solar Cell Performance of Boron-Containing Polyaromatic Compound **8 in Combination with Donor Polymers PBDB-T and PCE10 (1:1)^a**

donor polymer	V_{OC} [V]	J_{SC} [mA cm ⁻²]	FF [%]	PCE ^b [%]
PBDB-T	0.94 ± 0.01	-3.26 ± 0.07	36 ± 1	1.1 ± 0.1 (1.2)
PCE10	0.87 ± 0.01	-8.44 ± 0.07	40 ± 1	2.9 ± 0.1 (3.1)

^aStatistical data taken from 6 independent devices under 1000 W m⁻² AM1.5G illumination in the device architecture ITO/ZnO/BHJ/MoO₃/Al. ^bMaximum PCEs in parentheses.

CONCLUSION

We have synthesized core- and periphery-tuned boron-containing polybenzenoid PAHs via a facile and general C–H borylation strategy. Moreover, we have successfully converted so-formed borinic acids to B-mesityl substituted compounds. This approach has allowed the synthesis of ten boron-doped PAHs, including large and hitherto unknown doubly boron-doped anthranthrenes and triangulenes, that are stable under ambient conditions. X-ray crystallographic studies have revealed π -scaffold accessibility of compounds **2**, **4b**, and **5** as evidenced by intimate π – π stacking.

Although often advertised as electron acceptors for optoelectronic applications, the LUMO levels of boron-doped PAHs have lagged somewhat behind more established molecules such as PC₆₁BM ($E_{1/2} = -1.17$ V, $E_{LUMO} = -3.99$ eV).¹⁶ We have used structural tuning in conjunction with electrochemical studies to obtain four boron-doped PAHs (**4b**, **7**, **8**, and **9**) with LUMO energy levels comparable to or lower than that of PC₆₁BM. Diboraperylene **8** is to our knowledge the most readily reduced ambient stable boron-doped PAH yet reported ($E_{1/2} = -1.07$ V, $E_{LUMO} = -4.08$ eV).¹⁶ We have also found that the core structures corresponding to the lowest LUMO compounds did not correspond to the largest π -surfaces or to core structures bearing the largest proportion boron per carbon. These results suggest that ambitiously large or excessively boron-doped targets may not necessarily lead to desirable low LUMO levels. Rather, screening of core structures experimentally or computationally and further tuning properties with the more predictable electronic effects of periphery substituents presents a more tactful approach. For this reason, the facile access to different core structures provided by our synthetic methodology is beneficial.

Compounds **1–10** are typified by visible range absorptions which may suggest potential light-harvesting advantages over weakly absorbing compounds (like PC₆₁BM) in photovoltaic applications.^{9a} Furthermore, the ability to easily and independently tune both visible-light absorption and electrochemical reduction potentials contrasts with the more fixed properties of the fullerenes. Compounds **1–10** also show emissions in the visible to NIR regions with quantum yields as high as 95%. Both of these properties are appealing for prospective boron-doped PAH OLED^{3a} or sensing applications.²³

Finally, the lowest-LUMO energy level compound synthesized herein, **8**, could be implemented in OTFTs exhibiting n-type charge carrier mobilities of 3×10^{-3} cm² V⁻¹ s⁻¹ and implemented as an acceptor in combination with donor polymers in BHJ solar cells with PCEs up to 3%. This latter application represents the first use of a PAH with precise, electron-deficient three-coordinate boron-doping of the carbon scaffold as an acceptor material in organic photovoltaics. These

results encourage the exploration of small molecules bearing boron-doped polyaromatic carbon π -cores as new candidates for nonfullerene acceptors in organic solar cells.

In conclusion, our facile, general C–H borylation synthesis has allowed significant manipulation of boron-containing PAH properties through structural tuning. This has provided both insight on structure–property relationships and allowed optimization of desired properties toward organic electronic applications.

ASSOCIATED CONTENT

Supporting Information

The Supporting Information is available free of charge on the ACS Publications website at DOI: 10.1021/jacs.9b04675.

Experimental details on synthetic procedures, NMR spectroscopy, UV–vis and fluorescence spectroscopy, cyclic voltammetry, X-ray crystallography and computations (PDF)

Crystal data for 9,10-bis(2,3,4,5,6-pentafluorostyryl)-anthracene (CIF)

Crystal data for compound **2** (CIF)

Crystal data for compound **4b** (CIF)

Crystal data for compound **5** (CIF)

Crystal data for compound **8** (CIF)

AUTHOR INFORMATION

Corresponding Author

*wuerthner@uni-wuerzburg.de

ORCID

Frank Würthner: 0000-0001-7245-0471

Author Contributions

[§]JMF and CM contributed equally.

Notes

The authors declare no competing financial interest.

ACKNOWLEDGMENTS

We thank the Alexander von Humboldt foundation for a postdoctoral stipend for J.M.F. We thank Dr. Hagen Klauk and Dr. Ute Zschieschang (MPI für Festkörperforschung, Stuttgart) for providing us with TPA modified substrates.

REFERENCES

- (1) (a) Novoselov, K. S.; Geim, A. K.; Morozov, S. V.; Jiang, D.; Zhang, Y.; Dubonos, S. V.; Grigorieva, I. V.; Firsov, A. A. Electric Field Effect in Atomically Thin Carbon Films. *Science* **2004**, *306*, 666–669. (b) Allen, M. J.; Tung, V. C.; Kaner, R. B. Honeycomb Carbon: A Review of Graphene. *Chem. Rev.* **2010**, *110*, 132–145.
- (2) Narita, A.; Wang, X.-Y.; Feng, X.; Müllen, K. New advances in nanographene chemistry. *Chem. Soc. Rev.* **2015**, *44*, 6616–6643.
- (3) (a) Von Grothuss, E.; John, A.; Kaese, T.; Wagner, M. Doping Polycyclic Aromatics with Boron for Superior Performance in Materials Science and Catalysis. *Asian J. Org. Chem.* **2018**, *7*, 37–53. (b) Sępień, M.; Gońka, E.; Żyła, M.; Sprutta, N. Heterocyclic Nanographenes and Other Polycyclic Heteroaromatic Compounds: Synthetic Routes, Properties, and Applications. *Chem. Rev.* **2017**, *117*, 3479–3716. (c) Ji, L.; Griesbeck, S.; Marder, T. B. Recent developments in and perspectives on three-coordinate boron materials: a bright future. *Chem. Sci.* **2017**, *8*, 846–863. (d) Agnoli, S.; Favaro, M. Doping graphene with boron: a review of synthesis methods, physicochemical characterization, and emerging applications. *J. Mater. Chem. A* **2016**, *4*, S002–S025. (e) Escande, A.; Ingleson, M. J. Fused polycyclic aromatics incorporating boron in the core: fundamentals and applications. *Chem. Commun.* **2015**, *51*,

6257–6274. (f) Jäkle, F. Advances in the Synthesis of Organoborane Polymers for Optical, Electronic, and Sensory Applications. *Chem. Rev.* **2010**, *110*, 3985–4022.

(4) (a) Yamaguchi, S.; Wakamiya, A. Boron as a key component for new π -electron materials. *Pure Appl. Chem.* **2006**, *78*, 1413–1424.

(b) Møllerup, S. K.; Wang, S. Boron-Doped Molecules for Optoelectronics. *Trends Chem.* **2019**, *1*, 77–89.

(5) (a) Chen, J.; Kampf, J. W.; Ashe, A. J. Syntheses and Structures of 6,13-Dihydro-6,13-diborapentacenes: π -Stacking in Heterocyclic Analogues of Pentacene. *Organometallics* **2008**, *27*, 3639–3641.

(b) Wood, T. K.; Piers, W. E.; Keay, B. A.; Parvez, M. 9-Boraanthracene Derivatives Stabilized by N-Heterocyclic Carbenes. *Angew. Chem., Int. Ed.* **2009**, *48*, 4009–4012. (c) Wood, T. K.; Piers, W. E.; Keay, B. A.; Parvez, M. Synthesis and Comparative Characterization of 9-Boraanthracene, 5-Boranaphthacene, and 6-Borapentacene Stabilized by the H₂IMes Carbene. *Chem. - Eur. J.* **2010**, *16*, 12199–12206. (d) Dou, C.; Saito, S.; Matsuo, K.; Hisaki, I.; Yamaguchi, S. A Boron-Containing PAH as a Substructure of Boron-Doped Graphene. *Angew. Chem., Int. Ed.* **2012**, *51*, 12206–12210.

(e) Schickedanz, K.; Trageser, T.; Bolte, M.; Lerner, H.-W.; Wagner, M. A boron-doped helicene as a highly soluble, benchtop-stable green emitter. *Chem. Commun.* **2015**, *51*, 15808–15810. (f) Hertz, V. M.; Ando, N.; Hirai, M.; Bolte, M.; Lerner, H.-W.; Yamaguchi, S.; Wagner, M. Steric Shielding vs Structural Constraint in a Boron-Containing Polycyclic Aromatic Hydrocarbon. *Organometallics* **2017**, *36*, 2512–2519. (g) Kaese, T.; Hübner, A.; Bolte, M.; Lerner, H.-W.; Wagner, M. Forming B-B Bonds by the Controlled Reduction of a Tetraaryl-diborane(6). *J. Am. Chem. Soc.* **2016**, *138*, 6224–6233.

(h) Miyamoto, F.; Nakatsuka, S.; Yamada, K.; Nakayama, K.-I.; Hatakeyama, T. Synthesis of Boron-Doped Polycyclic Aromatic Hydrocarbons by Tandem Intramolecular Electrophilic Arene Borylation. *Org. Lett.* **2015**, *17*, 6158–6161. (i) Zhou, Z.; Wakamiya, A.; Kushida, T.; Yamaguchi, S. Planarized Triarylboranes: Stabilization by Structural Constraint and Their Plane-to-Bowl Conversion. *J. Am. Chem. Soc.* **2012**, *134*, 4529–4532. (j) Hertz, V. M.; Bolte, M.; Lerner, H.-W.; Wagner, M. Boron-Containing Polycyclic Aromatic Hydrocarbons: Facile Synthesis of Stable, Redox-Active Luminophores. *Angew. Chem., Int. Ed.* **2015**, *54*, 8800–8804. (k) John, A.; Bolte, M.; Lerner, H.-W.; Wagner, M. A Vicinal Electrophilic Diborylation Reaction Furnishes Doubly Boron-Doped Polycyclic Aromatic Hydrocarbons. *Angew. Chem., Int. Ed.* **2017**, *56*, 5588–5592. (l) Crossley, D. L.; Kahan, R. J.; Endres, S.; Warner, A. J.; Smith, R. A.; Cid, J.; Dunsford, J. J.; Jones, J. E.; Vitorica-Yrezabal, I.; Ingleson, M. J. A modular route to boron doped PAHs by combining borylative cyclisation and electrophilic C-H borylation. *Chem. Sci.* **2017**, *8*, 7969–7977. (m) Kahan, R. J.; Crossley, D. L.; Cid, J.; Radcliffe, J. E.; Woodward, A. W.; Fasano, V.; Endres, S.; Whitehead, G. F. S.; Ingleson, M. J. Generation of a series of B_n fused oligo-naphthalenes (n = 1 to 3) from a B₁-polycyclic aromatic hydrocarbon. *Chem. Commun.* **2018**, *54*, 9490–9493.

(n) Kushida, T.; Shirai, S.; Ando, N.; Okamoto, T.; Ishii, H.; Matsui, H.; Yamagishi, M.; Uemura, T.; Tsurumi, J.; Watanabe, S.; Takeya, J.; Yamaguchi, S. Boron-Stabilized Planar Neutral π -Radicals with Well-Balanced Ambipolar Charge-Transport Properties. *J. Am. Chem. Soc.* **2017**, *139*, 14336–14339. (o) Shuto, A.; Kushida, T.; Fukushima, T.; Kaji, H.; Yamaguchi, S. π -Extended Planarized Triphenylboranes with Thiophene Spacers. *Org. Lett.* **2013**, *15*, 6234–6237.

(6) Hertz, V. M.; Lerner, H.-W.; Wagner, M. Ru-Catalyzed Benzannulation Leads to Luminescent Boron-Containing Polycyclic Aromatic Hydrocarbons. *Org. Lett.* **2015**, *17*, 5240–5243.

(7) (a) Kawai, S.; Saito, S.; Osumi, S.; Yamaguchi, S.; Foster, A. S.; Spijker, P.; Meyer, E. Atomically controlled substitutional boron-doping of graphene nanoribbons. *Nat. Commun.* **2015**, *6*, 8098. (b) Cloke, R. R.; Marangoni, T.; Nguyen, G. D.; Joshi, T.; Rizzo, D. J.; Bronner, C.; Cao, T.; Louie, S. G.; Crommie, M. F.; Fischer, F. R. Site-Specific Substitutional Boron Doping of Semiconducting Armchair Graphene Nanoribbons. *J. Am. Chem. Soc.* **2015**, *137*, 8872–8875.

(8) (a) Matsuo, K.; Saito, S.; Yamaguchi, S. Photodissociation of B-N Lewis Adducts: A Partially Fused Trinaphthylborane with Dual Fluorescence. *J. Am. Chem. Soc.* **2014**, *136*, 12580–12583. (b) Kushida, T.; Shuto, A.; Yoshio, M.; Kato, T.; Yamaguchi, S. A Planarized Triphenylborane Mesogen: Discotic Liquid Crystals with Ambipolar Charge-Carrier Transport Properties. *Angew. Chem., Int. Ed.* **2015**, *54*, 6922–6925. (c) Matsuo, K.; Saito, S.; Yamaguchi, S. A Soluble Dynamic Complex Strategy for the Solution-Processed Fabrication of Organic Thin-Film Transistors of a Boron-Containing Polycyclic Aromatic Hydrocarbon. *Angew. Chem., Int. Ed.* **2016**, *55*, 11984–11988. (d) Osumi, S.; Saito, S.; Dou, C.; Matsuo, K.; Kume, K.; Yoshikawa, H.; Awaga, K.; Yamaguchi, S. Boron-doped nanographene: Lewis acidity, redox properties, and battery electrode performance. *Chem. Sci.* **2016**, *7*, 219–227. (e) John, A.; Bolte, M.; Lerner, H.-W.; Meng, G.; Wang, S.; Peng, T.; Wagner, M. Doubly boron-doped pentacenes as emitters for OLEDs. *J. Mater. Chem. C* **2018**, *6*, 10881–10887.

(9) (a) Yan, C.; Barlow, S.; Wang, Z.; Yan, H.; Jen, A. K. Y.; Marder, S. R.; Zhan, X. Non-fullerene acceptors for organic solar cells. *Nat. Rev. Mater.* **2018**, *3*, 18003. (b) Hummelen, J. C.; Knight, B. W.; LePeq, F.; Wudl, F.; Yao, J.; Wilkins, C. L. Preparation and Characterization of Fulleroid and Methanofullerene Derivatives. *J. Org. Chem.* **1995**, *60*, 532–538. (c) Würthner, F.; Stolte, M. Naphthalene and perylene diimides for organic transistors. *Chem. Commun.* **2011**, *47*, 5109–5115. (d) Nowak-Król, A.; Shoyama, K.; Stolte, M.; Würthner, F. Naphthalene and perylene diimides - better alternatives to fullerenes for organic electronics? *Chem. Commun.* **2018**, *54*, 13763–13772.

(10) Farrell, J. M.; Schmidt, D.; Grande, V.; Würthner, F. Synthesis of a Doubly Boron-Doped Perylene through NHC-Borenium Hydroboration/C-H Borylation/Dehydrogenation. *Angew. Chem., Int. Ed.* **2017**, *56*, 11846–11850.

(11) (a) Kölle, P.; Nöth, H. The chemistry of borinium and borenium ions. *Chem. Rev.* **1985**, *85*, 399–418. (b) Piers, W. E.; Bourke, S. C.; Conroy, K. D. Borinium, Borenium, and Boronium Ions: Synthesis, Reactivity, and Applications. *Angew. Chem., Int. Ed.* **2005**, *44*, 5016–5036. (c) De Vries, T. S.; Prokofjevs, A.; Vedejs, E. Cationic Tricoordinate Boron Intermediates: Borenium Chemistry from the Organic Perspective. *Chem. Rev.* **2012**, *112*, 4246–4282.

(12) (a) Prokofjevs, A.; Boussonniere, A.; Li, L.; Bonin, H.; Lacôte, E.; Curran, D. P.; Vedejs, E. Borenium ion catalyzed hydroboration of alkenes with N-heterocyclic carbene-boranes. *J. Am. Chem. Soc.* **2012**, *134*, 12281–12288. (b) De Vries, T. S.; Prokofjevs, A.; Harvey, J. N.; Vedejs, E. Superelectrophilic Intermediates in Nitrogen-Directed Aromatic Borylation. *J. Am. Chem. Soc.* **2009**, *131*, 14679–14687. (c) Farrell, J. M.; Stephan, D. W. Planar N-Heterocyclic Carbene Diarylborenium Ions: Synthesis by Cationic Borylation and Reactivity with Lewis Bases. *Angew. Chem., Int. Ed.* **2015**, *54*, 5214–5217. (d) Özgün, T.; Chen, G.-Q.; Daniliuc, C. G.; McQuilken, A. C.; Warren, T. H.; Knitsch, R.; Eckert, H.; Kehr, G.; Erker, G. Unsaturated Vicinal Frustrated Lewis Pair Formation by Electrocyclic Ring Closure and Their Reaction with Nitric Oxide. *Organometallics* **2016**, *35*, 3667–3680.

(13) Curran, D. P.; Solovye, A.; Brahmi, M. M.; Fensterbank, L.; Malacria, M.; Lacôte, E. Synthesis and Reactions of N-Heterocyclic Carbene Boranes. *Angew. Chem., Int. Ed.* **2011**, *50*, 10294–10317.

(14) An alternative synthesis for 1-boraphenalenenes has been recently described: Kahan, R. J.; Crossley, D. L.; Cid, J.; Radcliffe, J. E.; Ingleson, M. J. Synthesis, Characterization, and Functionalization of 1-Boraphenalenenes. *Angew. Chem., Int. Ed.* **2018**, *57*, 8084–8088.

(15) (a) Pavliček, N.; Mistry, A.; Majzik, Z.; Moll, N.; Meyer, G.; Fox, D. J.; Gross, L. Synthesis and characterization of triangulene. *Nat. Nanotechnol.* **2017**, *12*, 308–311. (b) Clar, E.; Stewart, D. G. Aromatic Hydrocarbons. LXV. Triangulene Derivatives. *J. Am. Chem. Soc.* **1953**, *75*, 2667–2672.

(16) Calculated according to the equation: $E_{\text{LUMO}} = -e(E_{1/2 \text{ red}}) - 5.15 \text{ eV}$. Adapted from: Cardona, C. M.; Li, W.; Kaifer, A. E.; Stockdale, D.; Bazan, G. C. Electrochemical Considerations for Determining Absolute Frontier Orbital Energy Levels of Conjugated

Polymers for Solar Cell Applications. *Adv. Mater.* **2011**, *23*, 2367–2371.

(17) Filippetti, A. Electron affinity in density-functional theory in the local-spin-density approximation. *Phys. Rev. A: At., Mol., Opt. Phys.* **1998**, *57*, 914–919.

(18) Birks, J. B. *Photophysics of Aromatic Molecules*; Wiley-Interscience: London, 1970.

(19) Berlman, I. B. *Handbook of Fluorescence Spectra of Aromatic Molecules*; Academic Press: London, 1965.

(20) Shah, B. K.; Neckers, D. C.; Shi, J.; Forsythe, E. W.; Morton, D. Photophysical Properties of Anthanthrene-Based Tunable Blue Emitters. *J. Phys. Chem. A* **2005**, *109*, 7677–7681.

(21) Exocyclic three-coordinate boron has been incorporated in polymeric acceptors and as a linking moiety for small-molecule acceptors in OPVs, see: (a) Cataldo, S.; Fabiano, S.; Ferrante, F.; Previti, F.; Patanè, S.; Pignataro, B. Organoboron Polymers for Photovoltaic Bulk Heterojunctions. *Macromol. Rapid Commun.* **2010**, *31*, 1281–1286. (b) Meng, B.; Ren, Y.; Liu, J.; Jäkle, F.; Wang, L. p- π Conjugated Polymers Based on Stable Triarylborane with n-Type Behavior in Optoelectronic Devices. *Angew. Chem., Int. Ed.* **2018**, *57*, 2183–2187. (c) Welsh, T. A.; Laventure, A.; Alahmadi, A. F.; Zhang, G.; Baumgartner, T.; Zou, Y.; Jäkle, F.; Welch, G. C. Borane Incorporation in a Non-Fullerene Acceptor To Tune Steric and Electronic Properties and Improve Organic Solar Cell Performance. *ACS Appl. Energy Mater.* **2019**, *2*, 1229–1240.

(22) Four-coordinate boron moieties have been included in acceptor materials for OPVs, for example: (a) Gommans, H.; Aernouts, T.; Verreert, B.; Heremans, P.; Medina, A.; Claessens, C. G.; Torres, T. Perfluorinated Subphthalocyanine as a New Acceptor Material in a Small-Molecule Bilayer Organic Solar Cell. *Adv. Funct. Mater.* **2009**, *19*, 3435–3439. (b) Poe, A. M.; Della Pelle, A. M.; Subrahmanyam, A. V.; White, W.; Wantz, G.; Thayumanavan, S. Small molecule BODIPY dyes as non-fullerene acceptors in bulk heterojunction organic photovoltaics. *Chem. Commun.* **2014**, *50*, 2913–2915. (c) Dou, C.; Ding, Z.; Zhang, Z.; Xie, Z.; Liu, J.; Wang, L. Developing Conjugated Polymers with High Electron Affinity by Replacing a C-C Unit with a B-N Unit. *Angew. Chem., Int. Ed.* **2015**, *54*, 3648–3652.

(23) Wade, C. R.; Broomsgrove, A. E. J.; Aldridge, S.; Gabbai, F. P. Fluoride Ion Complexation and Sensing Using Organoboron Compounds. *Chem. Rev.* **2010**, *110*, 3958–3984.